Eur. J. Mineral.
PrePub DOI: 10.1127/ejm/2016/0028-2527

PrePub Article

Crystal structure of bassetite and saléeite: new insight into autunite-group minerals

FABRICE DAL BO[1,*], FRÉDÉRIC HATERT[1], FLORIAS MEES[2], SIMON PHILIPPO[3], MAXIME BAIJOT[1] and FRANÇOIS FONTAINE[4]

[1] Laboratoire de Minéralogie, B18, Université de Liège, 4000 Liège, Belgium
*Corresponding author, e-mail: fdalbo@ulg.ac.be
[2] Royal Museum for Central Africa, 13 Leuvensesteenweg, 3080 Tervuren, Belgium
[3] Section Minéralogie, Musée national d'histoire naturelle, Rue Münster 25, 2160 Luxembourg, Grand-Duché de Luxembourg
[4] AGEs, Département de Géologie, B18, Université de Liège, 4000, Liège, Belgium

Abstract: The crystal structures of two autunite-group minerals have been solved recently. The crystal structure of bassetite, $Fe^{2+}[(UO_2)(PO_4)]_2(H_2O)_{10}$, from the type locality in Cornwall, United Kingdom (Basset Mines) was solved for the first time. Bassetite is monoclinic, space group $P2_1/n$, a = 6.961(1), b = 20.039(2), c = 6.974(1) Å and β = 90.46(1)°. The crystal structure of saléeite, $Mg[(UO_2)(PO_4)]_2(H_2O)_{10}$, from Shinkolobwe, Democratic Republic of Congo, was also solved. Saléeite is monoclinic, space group $P2_1/n$, a = 6.951(1), b = 19.942(1), c = 6.967(1) Å and β = 90.58(1)°. The crystal structure investigation of bassetite (R_1 = 0.0658 for 1879 observed reflections with $|F_o| \geq 4\sigma_F$) and saléeite (R_1 = 0.0307 for 1990 observed reflections with $|F_o| \geq 4\sigma_F$) confirms that both minerals are topologically identical and that bassetite contains ten water molecules per formula unit. Their structure contains autunite-type sheets, $[(UO_2)(PO_4)]^-$, consisting of corner-sharing UO_6 square bipyramids and PO_4 tetrahedra. Iron and magnesium are surrounded by water molecules to form $Fe(H_2O)_6$ or $Mg(H_2O)_6$ octahedra located in interlayer, between the autunite-type sheets. Two isolated independent water molecules are also located in interlayer. Energy-dispersive X-ray spectroscopy analysis confirmed the chemical composition obtained from structure refinement. These new data prompt a re-assessment of minerals of the autunite and meta-autunite groups.

Key-words: bassetite; saléeite; crystal structure; solid-solution; autunite group; uranyl phosphate hydrate; Basset Mines; Shinkolobwe.

1. Introduction

The autunite and meta-autunite groups are the main groups of uranyl phosphates and arsenates. Together, they represent about forty mineral species which show the typical autunite-type sheet and which contain a wide variety of interstitial mono-, di-, or trivalent cations (Krivovichev & Plášil, 2013). The crystal structures have been determined for approximately twenty of these minerals, and new species belonging to the autunite and meta-autunite groups continue to be reported, as shown by the recent discovery of metarauchite $Ni[(UO_2)(AsO_4)]_2(H_2O)_8$ (Plášil *et al.,* 2010a) and rauchite $Ni[(UO_2)(AsO_4)]_2(H_2O)_{10}$ (Pekov *et al*., 2012). Recent structural investigations have also been performed on saléeite $Mg[(UO_2)(PO_4)]_2(H_2O)_{10}$ (Yakubovich *et al.*, 2008) and on arsenuranospathite $Al[(UO_2)(AsO_4)]_2F(H_2O)_{20}$ (Dal Bo *et al*., 2015). The investigation of these minerals is of interest because they control the mobility and solubility of uranium in many geological environments. Due to their very low solubility products, uranyl phosphates and arsenates can behave as a trap for uranium in oxidation zones of uranium deposits (Murakami *et al.,* 1997), in soils contaminated by actinides (Buck *et al.,* 1996; Roh *et al.,* 2000), and in groundwater and wastewater systems (Fuller *et al.*, 2002; Jerden & Sinha, 2003; Grabias *et al.,* 2014).

In the present study, the crystal structure of bassetite from the type locality is presented for the first time, and the crystal structure of saléeite is described in order to highlight the solid-solution relationship between both species. Based on the obtained structural and chemical data, new considerations about the minerals of the autunite group are formulated.

2. Previous studies

Bassetite, $Fe^{2+}[(UO_2)(PO_4)]_2(H_2O)_n$, is one of the oldest known uranyl phosphates. Discovered in 1915 by

0935-1221/16/0028-2527 $ 5.85
DOI: 10.1127/ejm/2016/0028-2527

Hallimond in the Wheal Basset Mine, Cornwall, England, bassetite occurs usually as fan-like groups of tabular crystals. Optical properties show that the mineral is biaxial, and the morphological analyses, as well as the measurements of angles between crystal faces, indicate that the mineral has a pseudo-orthorhombic or a pseudo-tetragonal symmetry. Semi-quantitative spectrographic analyses performed by Frondel (1954) on the material collected by Hallimond (1915) confirm that bassetite contains only Fe, U and P as major elements. Its X-ray powder- diffraction pattern indicates that bassetite is closely related to saléeite, a Mg-bearing uranyl phosphate. The X-ray single-crystal study of bassetite by the Weissenberg method yielded the unit-cell parameters $a = 6.98(4)$, $b = 17.07(4)$, $c = 7.01(7)$ Å and $\beta = 90.32(5)^\circ$ (Frondel, 1954). Using the unit-cell parameters provided by Frondel (1954) for bassetite, Vochten *et al.* (1984) indexed the X-ray powder-diffraction pattern of synthetic bassetite in space group $P2_1/m$. The same authors also synthesized fully oxidized bassetite by reaction between synthetic bassetite and H_2O_2 at room temperature. The unit-cell parameters for fully oxidized synthetic bassetite are $a = 6.958(5)$, $b = 6.943(5)$, $c = 21.052(5)$ Å and $\beta = 90.90(5)^\circ$. The presence of Fe^{3+} in the structure of oxidized synthetic bassetite was confirmed by Mössbauer spectroscopy, whereby the oxidation process is considered to be $Fe^{2+}+H_2O \rightarrow Fe^{3+}+OH^-$ ($Fe^{2+}_{1-x}Fe^{3+}_x[(UO_2)(PO_4)]_2(OH)_x(H_2O)_n$ with $0 \leq x \leq 1$). Infrared spectroscopic analyses show a modification in the OH frequencies, in good agreement with Fe^{2+} oxidation. However, the substitution between H_2O and OH^- groups is not confirmed, as no modifications are observed in the region characteristic of OH^- groups (Vochten *et al.,* 1984).

Saléeite, $Mg[(UO_2)(PO_4)]_2(H_2O)_n$, was first described by Thoreau & Vaes (1932), from samples of the Shinkolobwe uranium mine, Katanga, Democratic Republic of Congo (DRC). Saléeite occurs as square or rectangular plates flattened on {001}, and generally forms aggregates of subparallel lamellae. The colour of the plates varies between canary-yellow to olive-green or brown. Mrose (1950) and Frondel (1951) presented new data for saléeite and nováčekite, the As-analogue of saléeite, from Schneeberg, Saxony, Germany and Mina da Quarta Seira, Sabugal, Portugal. Chemical analysis performed by Frondel (1951) on saléeite from Shinkolobwe and Portugal show that the composition of the mineral is close to the ideal formula with only a small amount of Pb and Al substituting for Mg. However, chemical analyses performed by Mrose (1950) on saléeite and nováčekite from Germany indicate that P and As are present in both minerals and that, therefore, a complete solid solution exists between saléeite and nováčekite. Frondel (1951) reported unit–cell parameters for saléeite from Portugal ($a = 7.01$ Å and $c = 19.84$ Å), whereas Mrose (1950) obtained the unit-cell parameters for saléeite from Schneeberg ($a = 6.980$ Å and $c = 19.813$ Å), with $I4/mmm$ as assumed space group. This tetragonal symmetry is in contradiction with the orthorhombic symmetry reported by Thoreau & Vaes (1932), and with the monoclinic symmetry reported by Schoep (1939). Reinvestigation of the saléeite holotype from Shinkolobwe by Piret & Deliens (1980) shows that saléeite is monoclinic ($P2_1/n$) with a pseudo-tetragonal symmetry: $a = 6.971(10)$, $b = 6.973(10)$, $c = 19.935(15)$ Å and $\gamma = 90.2(2)^\circ$. Furthermore, thermal analysis of fully hydrated saléeite indicates the presence of 10.7 H_2O molecules per formula unit (*pfu*). Miller & Taylor (1986) solved for the first time the structure of saléeite in the monoclinic $P2_1/c$ space group, with $a = 6.951(3)$, $b = 19.948(8)$, $c = 9.896(4)$ Å and $\beta = 135.17(2)^\circ$. The structure model confirms that saléeite contains the autunite-type sheet, and shows that Mg occurs in a $Mg(H_2O)_6$ octahedron located between the uranyl-phosphate sheets. The structure model indicates also that saléeite contains 10 water molecules *pfu.* Yakubovich *et al.* (2008) have reported the structure of Fe- and As-rich saléeite from the Eduardo Mine, Minas Gerais, Brazil. This saléeite has the structural formula $(Mg_{0.81}Fe_{0.19})[(UO_2)(P_{0.67}As_{0.33})O_4)]_2(H_2O)_{10}$, unit-cell parameters $a = 6.952(6)$, $b = 19.865(5)$, $c = 6.969(2)$ Å, $\beta = 90.806(4)^\circ$, and space group $P2_1/n$ (the change of space group, compared to Miller & Taylor (1986), is due to a different setting of the unit cell, with transformation matrix 1 0 0/0 1 0/−1 0 1). Their study clearly indicates isomorphism between saléeite and nováčekite (P-As), and also between saléeite and bassetite (Mg-Fe).

3. Experimental procedure

3.1. Sample description

The samples of bassetite studied are from the collections of the Musée Royal de l'Afrique Centrale (Royal Museum for Central Africa), in Tervuren, Belgium (sample references RGM 13739, 17341 and 13742). These specimens are from Basset Mines, Cornwall, United Kingdom (type locality), and were obtained from the British Museum and the Smithsonian Institution in 1980. Bassetite occurs as brown-yellow transparent platy crystals which are up to 0.5 mm in length (Fig. 1a). The crystals are flattened on (010) and show the {100}, {010}, and {001} forms. One perfect cleavage plane is observed along (010), as well as two other weaker cleavage planes parallel to (100) and (001). Unfortunately, only specimen 13742 gives suitable crystals for X-ray crystallographic analyses.

The sample containing saléeite was provided by Mr. Stéphane Puccio and is from Shinkolobwe, Katanga, Democratic Republic of Congo. Saléeite occurs as yellow transparent square plates showing the {100}, {010}, {001} and {110} forms (Fig. 1b). As also observed for bassetite, the (010) cleavage is perfect, with weaker cleavage planes parallel to (100) and (001). Saléeite forms intimate intergrowths with emerald-green platy crystals of torbernite. Identification of torbernite was confirmed by the unit-cell parameters obtained by single-crystal X-ray diffraction analysis. The contact between saléeite and torbernite is

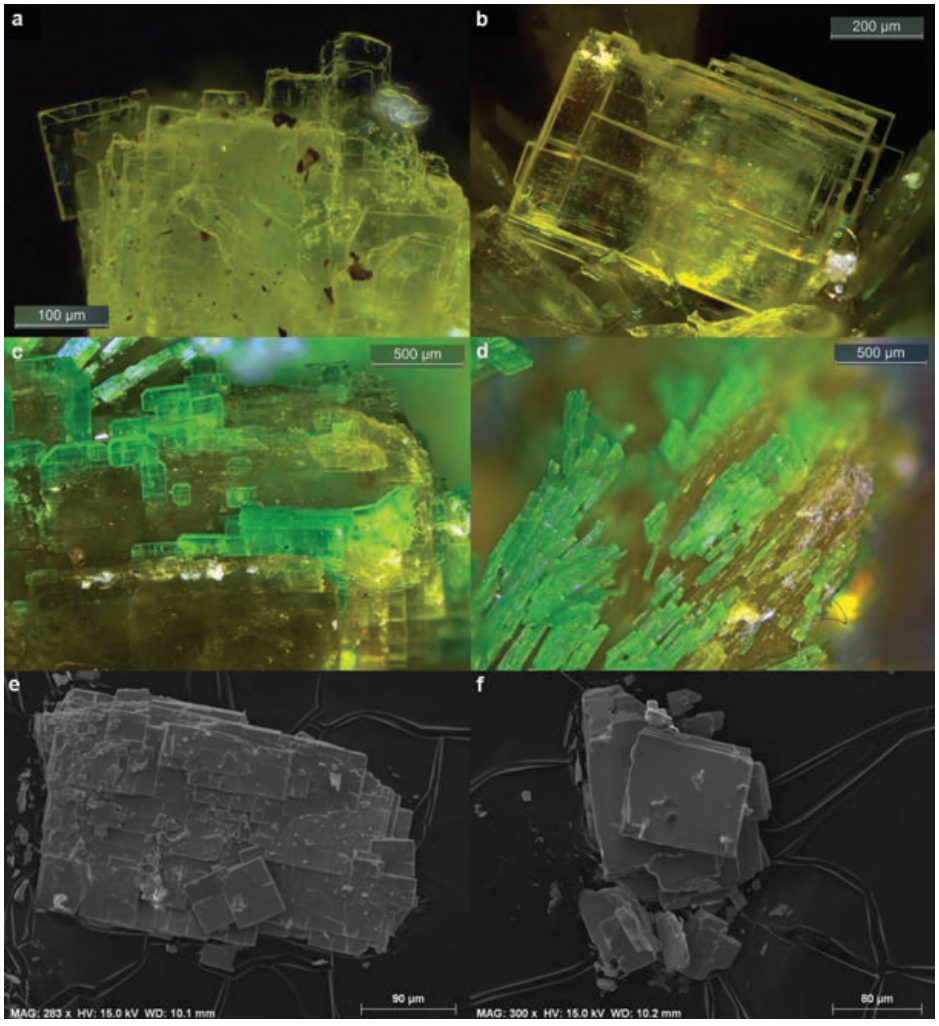

Fig. 1. Images of analyzed specimens. (a) yellow-transparent platy bassetite crystals (sample RGM 13742); (b) isolated yellow-transparent and platy saléeite crystals; (c), (d) intimate association between saléeite and torbernite, with sharp contacts; some torbernite crystals are surrounded by saléeite; (e), (f) backscattered-electron images of bassetite (e) and saléeite (f), showing prominent cleavage. Photographs (a) to (d) by R. Warin.

commonly very sharp. Figure 1d shows clearly alternating plates of yellow saléeite and green torbernite.

3.2. Chemical composition

Energy-dispersive X-ray spectroscopy (EDS) was used to confirm the chemical composition of bassetite and saléeite. The crystals were mounted on adhesive carbon tape, carbon-coated and analysed with an environmental scanning electron microscope (FEX XL30 ESEM-FEG) working in high vacuum mode, using 15 kV accelerating potential. The elements U, P, Fe, Mg and O were detected for all three bassetite samples, whereas only U, P, Mg and O were detected for saléeite (Fig. 2). No other elements, including As, were detected for bassetite or saléeite. The EDS analyses also confirm that the green mineral associated with saléeite is pure torbernite, as only Cu, P and U were detected.

3.3. Single-crystal X-ray diffraction

The single-crystal X-ray study of bassetite and saléeite was carried out with an Agilent Technologies Xcalibur four-circle diffractometer (kappa geometry), using Mo$K\alpha$ radiation ($\lambda = 0.71073$ Å, 40 kV, 40 mA), and equipped with an EOS CCD area detector. The data were corrected for Lorentz, polarization and absorption effects, the latter with an empirical method using the SCALE3 ABSPACK scaling algorithm included in the CrysAlisRED software package (Agilent Technologies, 2012). The crystal structure of bassetite and saléeite were solved by direct method with SHELXS and subsequently refined using SHELXL software (Sheldrick, 2008). For both minerals the diffraction patterns clearly indicate a centrosymmetric monoclinic cell with $a = 6.9612(4)$, $b = 20.039(2)$, $c = 6.9743(3)$ Å, $\beta = 90.465(5)^\circ$ for bassetite, and $a = 6.9516(3)$, $b = 19.942(1)$, $c = 6.9667(3)$ Å, $\beta = 90.586(4)^\circ$ for saléeite (Table 1). These results are in agreement with those

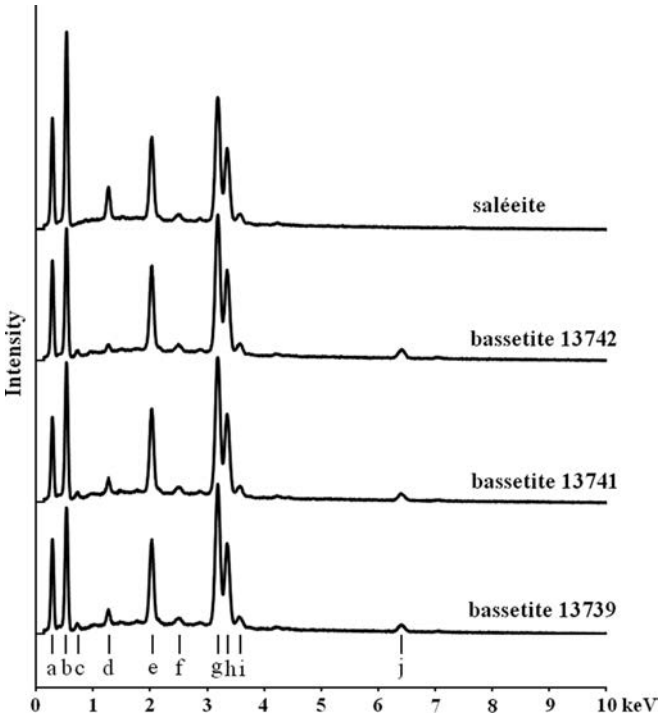

Fig. 2. Energy-dispersion X-ray emission spectra of bassetite and saléeite. The labelled EDS peaks correspond to the following X-ray lines: a, C*Kα*; b, O*Kα*; c, Fe*Kß*; d, *Mg*K*α*; e, P*Kα*; f, U*Mζ*; g, U*Mα*; h, U*Mß*; I, U*Mγ*; j, Fe*Kα*.

reported by Yakubovich *et al.* (2008) for Fe- and As-rich saléeite. Scattering curves for neutral atoms and anomalous dispersion correction were taken from the tables compiled by Wilson (1992).

3.4. Structure solution and refinement

The structures of bassetite and saléeite were solved by direct methods and were refined successfully on the basis of F^2 for all unique data in space group $P2_1/n$. Structure models including anisotropic displacement parameters for all non-H atoms converged and gave an agreement index ($R1$) of 12.56% for bassetite, and 3.21% for saléeite, calculated for the 1879 (bassetite) and 1990 (saléeite) observed unique reflections ($|F_o| \geq 4\sigma_F$). Due to the value of the β angle close to 90°, a pseudo-orthorhombic twin law [100/0−10/00-1] was applied, yielding an improvement of the agreement index (R1) to 6.58% for bassetite, and to 3.07% for saléeite. The application of this twin law greatly increases the quality of the refinement of the bassetite structure, and less strongly affects that of saléeite structure. The relative occupancy of the Fe site (bassetite) and Mg site (saléeite), as well as the relative occupancy of the P site in both structures, were refined assuming the absence of vacancies. The refinement of P site occupancy indicates that this site is fully occupied by phosphorus in both structures, which is

Table 1. Crystal data, data collection and refinement details for bassetite and saléeite.

	Bassetite	Saléeite
Ideal formula	$Fe^{2+}[(UO_2)(PO_4)]_2(H_2O)_{10}$	$Mg[(UO_2)(PO_4)]_2(H_2O)_{10}$
Locality	Basset Mines, UK	Shinkolobwe, DRC
a (Å)	6.9612(4)	6.9516(3)
b (Å)	20.039(2)	19.942(1)
c (Å)	6.9743(3)	6.9667(3)
β (°)	90.465(5)	90.586(4)
V (Å^3)	972.86(13)	965.76(8)
Space group	$P2_1/n$	$P2_1/n$
Z	2	2
D_{calc} (g.cm^{-3})	3.216	3.310
μ (mm^{-1})	17.608	17.408
F(000)	844	870
Radiation λ (Å)	Mo*Kα*, 0.71073	Mo*Kα*, 0.71073
Crystal size (mm)	0.19 × 0.11 × 0.02	0.22 × 0.09 × 0.05
Colour and habit	brown−yellow plate	yellow plate
Temperature (K)	293(2)	293(2)
θ range (°)	2.92−28.83	2.92−28.88
Index ranges	$-9 \leq h \leq 9-25, \leq k \leq 26-9, \leq l \leq 9$	$-8 \leq h \leq 8-24, \leq k \leq 25-9, \leq l \leq 8$
Total no. of reflections	8210	7542
Unique reflections	2318	2276
Observed reflections, $\|F_o\| \geq 4\sigma_F$	1879	1990
Twin matrix	[100/0−10/00−1]	[100/0−10/00−1]
Twin proportion (%)	0.19(4)	0.01(1)
Refined parameters	147	157
R_1, $\|F_o\| \geq 4\sigma_F$	0.0658	0.0307
R_1, all data	0.0841	0.0376
wR_2 (F^2), all data	0.1569	0.0736
GOF obs/all	1.034/1.030	1.081/1.076
$\Delta\sigma_{min}$ $\Delta\sigma_{max}$ (e/Å^3)	3.87−3.05	3.09−1.50

Table 2. Atom coordinates and anisotropic displacement parameters (Å^2) for bassetite from Basset Mines, United Kingdom.

	x	*y*	*z*	U_{eq}
Fe*	0	0.5	0	0.0251(18)
U	0.55105(11)	0.20834(4)	0.02029(11)	0.0157(2)
P	0.0529(8)	0.2510(2)	0.0228(8)	0.0164(9)
O1	0.554(2)	0.1210(8)	0.021(2)	0.024(3)
O2	0.544(2)	0.2953(7)	0.020(2)	0.022(3)
O3	0.017(2)	0.2945(8)	−0.1519(19)	0.020(3)
O4	0.0962(19)	0.2966(8)	0.195(2)	0.019(3)
O5	0.2349(19)	0.2049(7)	−0.018(2)	0.018(3)
O6	−0.117(2)	0.2069(8)	0.064(2)	0.022(3)
O7	−0.092(3)	0.4980(10)	0.282(3)	0.038(5)
O8	0.175(2)	0.5816(10)	0.068(3)	0.037(4)
O9	−0.229(3)	0.5713(10)	−0.071(3)	0.037(4)
O10	−0.424(3)	0.4275(13)	0.357(4)	0.058(6)
O11	0.533(3)	0.5853(12)	0.243(3)	0.049(5)
H7a	−0.12(4)	0.534(3)	0.34(2)	0.046
H7b	−0.16(3)	0.466(6)	0.32(2)	0.046
H8a	0.24(3)	0.594(7)	−0.028(19)	0.044
H8b	0.11(2)	0.614(5)	0.11(3)	0.044
H9a	−0.19(3)	0.598(7)	−0.16(2)	0.044
H9b	−0.26(3)	0.593(8)	0.029(13)	0.044
H10a	−0.43(4)	0.3851(16)	0.36(5)	0.070
H10b	−0.536(18)	0.443(13)	0.34(5)	0.070
H11a	0.42(2)	0.572(15)	0.20(4)	0.059
H11b	0.56(4)	0.562(14)	0.34(3)	0.059

	U_{11}	U_{22}	U_{33}	U_{23}	U_{13}	U_{12}
Fe	0.019(3)	0.030(3)	0.026(3)	0.001(3)	0.002(2)	−0.001(2)
U	0.0099(3)	0.0267(4)	0.0105(3)	0.0002(3)	0.0006(3)	0.0000(3)
P	0.0077(17)	0.033(3)	0.0087(18)	−0.002(2)	0.0009(18)	0.001(2)
O1	0.010(5)	0.050(9)	0.012(5)	0.002(8)	−0.006(6)	0.000(7)
O2	0.008(5)	0.045(8)	0.012(5)	0.002(8)	0.000(6)	−0.006(7)
O3	0.024(8)	0.027(8)	0.010(6)	0.002(6)	0.007(6)	0.003(7)
O4	0.008(7)	0.030(9)	0.017(7)	0.002(7)	0.000(5)	−0.004(6)
O5**	–	–	–	–	–	–
O6**	–	–	–	–	–	–
O7	0.025(10)	0.037(11)	0.050(12)	−0.004(9)	0.004(8)	0.005(8)
O8	0.018(8)	0.049(12)	0.044(12)	−0.003(9)	0.004(7)	−0.004(8)
O9	0.027(9)	0.045(12)	0.039(11)	0.000(9)	0.000(8)	−0.001(9)
O10	0.043(13)	0.053(15)	0.079(16)	0.020(13)	−0.010(12)	0.003(11)
O11	0.044(12)	0.062(15)	0.042(11)	−0.005(10)	−0.010(10)	−0.003(12)

* Refined Fe site occupancy: 0.64(3) Fe^{2+}+0.36(3) Mg. ** Refined with isotropic atomic displacement parameters.

consistent with the absence of As in both minerals. As the EDS analyses detected no elements that can substitute for Fe and Mg, these cations were refined together, leading to an occupancy of 0.64 Fe and 0.36 Mg for the Fe site of bassetite, and 0.97 Mg and 0.03 Fe for the Mg site of saléeite. Hydrogen atoms were located by the difference Fourier syntheses and subsequently refined using soft constraints on bond lengths (0.85 Å with a weight of 0.02), and their isotropic displacement parameters were set to $1.2U_{eq}$ of the parent (donor) O atoms (Tables 2 and 3). The refinement of the bassetite (saléeite) structure converged with final indices of agreement R_1 = 0.0841 (0.0376) and wR_2 = 0.1569 (0.0736), for all data using structure-factor weights assigned during least-squares refinement. Selected interatomic bond distances and the bond-valence sums (BVS) are given in Tables 4-7. The BVS were calculated with the parameters of Brown & Altermatt (1985) for Fe^{2+}, Mg, P and H, and those of Burns *et al.* (1997) for U^{6+}. In the bassetite structure, the BVS is 2.04 valence units (vu) for the Fe site, 6.16 *vu* for the U site, and 4.96 *vu* for the P site; for saléeite, it is 2.18 *vu* for the Mg site, 5.99 *vu* for the U site, and 4.94 *vu* for the P site. The BVS values for oxygen atoms in both structures range from 1.66 to 2.13 *vu,* and for hydrogen atoms from 0.85 to 0.97 *vu* (Tables 6 and 7). Further details of the crystal-structure investigation are available from the Fachinformationszentrum Karlsruhe, 76344 Eggenstein-Leopoldshafen, Germany, on quoting the depository number CSD-430600 (bassetite) and CSD-430599 (saléeite), the names of the authors and the citation of the paper.

Table 3. Atom coordinates and anisotropic displacement parameters (Å^2) for saléeite from Shinkolobwe, DRC.

	x	*y*	*z*	U_{eq}		
Mg*	0	0.5	0	0.0245(13)		
U	0.55094(3)	0.20834(1)	0.02137(3)	0.01428(9)		
P	0.0536(2)	0.25161(10)	0.0250(3)	0.0152(4)		
O1	0.5553(7)	0.1194(3)	0.0233(7)	0.0211(11)		
O2	0.5449(7)	0.2968(3)	0.0193(7)	0.0230(12)		
O3	0.0155(8)	0.2962(3)	−0.1519(7)	0.0209(11)		
O4	0.0971(8)	0.2984(3)	0.1952(7)	0.0211(11)		
O5	0.2267(7)	0.2047(3)	−0.0147(8)	0.0232(12)		
O6	−0.1214(7)	0.2081(3)	0.0669(8)	0.0219(11)		
O7	−0.0949(9)	0.4966(3)	0.2766(9)	0.0342(14)		
O8	0.1702(9)	0.5799(3)	0.0663(10)	0.0350(14)		
O9	−0.2247(9)	0.5688(3)	−0.0715(9)	0.0330(14)		
O10	−0.4307(12)	0.4275(4)	0.3589(12)	0.056(2)		
O11	0.5286(9)	0.5859(4)	0.2377(9)	0.0386(15)		
H7a	−0.093(12)	0.531(2)	0.348(8)	0.041		
H7b	−0.185(10)	0.471(3)	0.312(8)	0.041		
H8a	0.263(9)	0.586(3)	−0.009(10)	0.042		
H8b	0.112(7)	0.6164(16)	0.086(13)	0.042		
H9a	−0.183(8)	0.6071(17)	−0.104(12)	0.040		
H9b	−0.304(10)	0.574(3)	0.020(8)	0.040		
H10a	−0.413(15)	0.393(4)	0.293(15)	0.067		
H10b	−0.539(9)	0.445(5)	0.334(17)	0.067		
H11a	0.409(4)	0.589(5)	0.210(12)	0.047		
H11b	0.542(12)	0.564(5)	0.342(8)	0.047		
	U_{11}	U_{22}	U_{33}	U_{23}	U_{13}	U_{12}
Mg	0.025(2)	0.025(2)	0.024(2)	−0.0021(15)	0.0021(14)	−0.0004(14)
U	0.01158(14)	0.02034(15)	0.01091(13)	0.00039(10)	0.00059(9)	0.00003(10)
P	0.0120(8)	0.0238(10)	0.0099(8)	0.0007(7)	0.0009(6)	−0.0002(7)
O1	0.021(2)	0.024(3)	0.019(2)	0.000(2)	0.001(2)	0.000(2)
O2	0.021(3)	0.029(3)	0.019(3)	0.000(2)	0.002(2)	−0.001(2)
O3	0.025(3)	0.028(3)	0.010(2)	0.000(2)	−0.002(2)	0.003(2)
O4	0.025(3)	0.028(3)	0.011(2)	−0.003(2)	0.002(2)	−0.003(2)
O5	0.012(2)	0.030(3)	0.027(3)	−0.001(2)	−0.007(2)	0.002(2)
O6	0.008(2)	0.034(3)	0.024(3)	0.000(2)	0.003(2)	−0.002(2)
O7	0.041(4)	0.033(4)	0.029(3)	−0.004(3)	0.006(3)	−0.004(3)
O8	0.032(3)	0.028(3)	0.045(4)	−0.007(3)	0.004(2)	−0.004(3)
O9	0.029(3)	0.035(4)	0.035(3)	0.001(3)	0.003(3)	0.000(3)
O10	0.062(5)	0.050(5)	0.056(5)	0.000(4)	0.001(4)	−0.014(4)
O11	0.035(3)	0.043(4)	0.037(4)	0.000(3)	−0.005(3)	0.003(3)

* Refined Mg site occupancy: 0.97(1) Mg + 0.03(1) Fe^{2+}.

4. Description of the structures

The crystal structure of saléeite has been described by Yakubovich *et al.* (2008); therefore only the structure of bassetite, which is isostructural with saléeite, will be described here in detail. The main structural feature of bassetite is the corrugated autunite-type sheet (Beintema, 1938), which also characterizes all other members of the autunite group. In bassetite, the sheets consist of corner-sharing $U^{6+}O_6$ square bipyramids and PO_4 tetrahedra, resulting in a $[(U^{6+}O_2)(PO_4)]^-$ unit. The negative charge of the sheets is balanced by one Fe^{2+} atom (bassetite) or one Mg atom (saléeite) located in the interlayer space of the structure (Fig. 3). Both Fe^{2+} and Mg occur in $M(H_2O)_6$ octahedra (M = Fe^{2+}, Mg) which are not directly connected to the polyhedra of the uranyl-phosphate sheets. The interlayer space of the structure also contains two symmetrically independent H_2O molecules, which are not directly coordinated to any metal-cation sites; however, they are linked through the H-bonds with $M(H_2O)_6$ octahedra and with oxygen atoms of the uranyl-phosphate sheets.

The H-bond network in the structure of bassetite consists of five independent water molecules, of which three are connected to Fe to form $Fe(H_2O)_6$ octahedra, and two are isolated in the interlayer space (Table 5). The water molecules around Fe (H_2O_7, H_2O_8 and H_2O_9) mainly form H-bonds with oxygen atoms of the uranyl-phosphate sheets, with O1 and O_2 which are part of the UO_2^{2+} uranyl ion and also with O3 and O4 which are part of the

Table 4. Bond distances (Å) for bassetite and saléeite.

	Bassetite	Saléeite
U-O1	1.75(1)	1.773(5)
U-O2	1.74(1)	1.764(5)
U-O3^{i}	2.30(1)	2.294(5)
U-O4^{ii}	2.30(1)	2.302(5)
U-O5	2.22(1)	2.267(5)
U-O6^{iii}	2.33(1)	2.296(5)
	1.74	1.77
	2.29	2.29
P-O3	1.52(1)	1.540(5)
P-O4	1.53(2)	1.536(5)
P-O5	159(1)	1.551(5)
P-O6	1.51(2)	1.525(5)
	1.54	1.54
M-O7	2.07(2)	2.044(6)
M-O7^{iv}	2.07(2)	2.044(6)
M-O8	2.09(2)	2.035(6)
M-O8^{iv}	2.09(2)	2.035(6)
M-O9	2.20(2)	2.134(6)
M-O9^{iv}	2.20(2)	2.134(6)
	2.12	2.07

Symmetry codes: (i) $x + 1/2, -y + 1/2, z + 1/2$; (ii) $x + 1/2, -y + 1/2, z - 1/2$; (iii) $x + 1, y, z$; (iv) $-x, -y + 1, -z$. * M = Fe or Mg.

corrugated sheets (Figs 4 and 5). These groups of water molecules also share H-bonds with isolated water molecules H_2O10 (O7-H7b ··· O10) and H_2O11 (O9-H9b ··· O11). These water molecules have H-bonds with O5 of the uranyl-phosphate sheet, and with H_2O8 and H_2O9 of the $Fe(H_2O)_6$ octahedra (Tables 5 and 6).

5. Discussion

5.1. Structural comparison with other members of the autunite group

The structure of saléeite was first refined by Miller & Taylor (1986) and afterwards by Yakubovich *et al.* (2008). Despite differences in unit-cell parameters, both studies propose the same structure model. In the present work, the structure of bassetite and saléeite were refined using the same space group as that reported by Yakubovich *et al.* (2008). The structure models of bassetite and saléeite are identical to that of Fe- and As-rich saléeite reported by Yakubovich *et al.* (2008). These observations indicate that a complete solid solution occurs between saléeite and bassetite (corresponding to $(Mg,Fe^{2+})[(UO_2)(AsO_4)]_2(H_2O)_{10}$), between saléeite and nováčekite $(Mg[(UO_2)((P,As)O_4)]_2(H_2O)_{10})$, and between bassetite and kahlerite $(Fe^{2+}[(UO_2)((P,As)O_4)]_2(H_2O)_{10})$.

Comparison with other minerals or synthetic compounds that contain the autunite-type sheet indicates that bassetite and saléeite have the same arrangement of water molecules in the interlayer space as the synthetic compounds $Mg[(UO_2)(AsO_4)]_2(H_2O)_{10}$ (equivalent of

Table 5. Hydrogen-bond geometry in the structures of bassetite and saléeite.

	Bassetite			
Bond	O–H (Å)	H ··· O (Å)	O ··· O (Å)	O–H ··· O (°)
O7–H7a ··· O1	0.85(11)	2.05(11)	2.83(3)	154(4)
O7–H7b ··· O10	0.84(16)	2.00(20)	2.76(4)	148(3)
O8–H8a ··· O2	0.85(16)	2.68(17)	3.21(3)	122(2)
O8–H8b ··· O3	0.85(14)	2.06(12)	2.88(3)	165(3)
O9–H9a ··· O4	0.85(13)	2.22(15)	2.94(3)	139(2)
O9–H9b ··· O11	0.86(15)	2.09(16)	2.77(3)	137(3)
O10–H10a ··· O5	0.85(5)	2.30(19)	3.00(3)	140(5)
O10–H10b ··· O9	0.85(16)	2.50(30)	3.12(4)	131(3)
O11–H11a ··· O8	0.88(19)	1.94(19)	2.77(3)	156(3)
O11–H11b ··· O10	0.80(30)	2.30(30)	2.91(4)	126(3)
	Saléeite			
Bond	O–H (Å)	H ··· O (Å)	O ··· O (Å)	O–H ··· O (°)
O7–H7a ··· O1	0.85(5)	1.99(5)	2.83(1)	169(1)
O7–H7b ··· O10	0.85(7)	1.95(7)	2.78(1)	166(1)
O8–H8a ··· O2	0.84(7)	2.69(7)	3.22(1)	121(1)
O8–H8b ··· O3	0.84(7)	2.05(1)	2.85(1)	175(2)
O9–H9a ··· O4	0.85(5)	2.08(5)	2.93(1)	176(1)
O9–H9b ··· O11	0.85(7)	1.94(7)	2.79(1)	176(1)
O10–H10a ··· O5	0.84(9)	2.55(9)	2.98(1)	113(1)
O10–H10b ··· O9	0.85(8)	2.46(9)	3.10(1)	133(2)
O11–H11a ··· O8	0.85(4)	1.94(5)	2.75(1)	159(2)
O11–H11b ··· O10	0.85(8)	2.24(7)	2.91(1)	136(1)

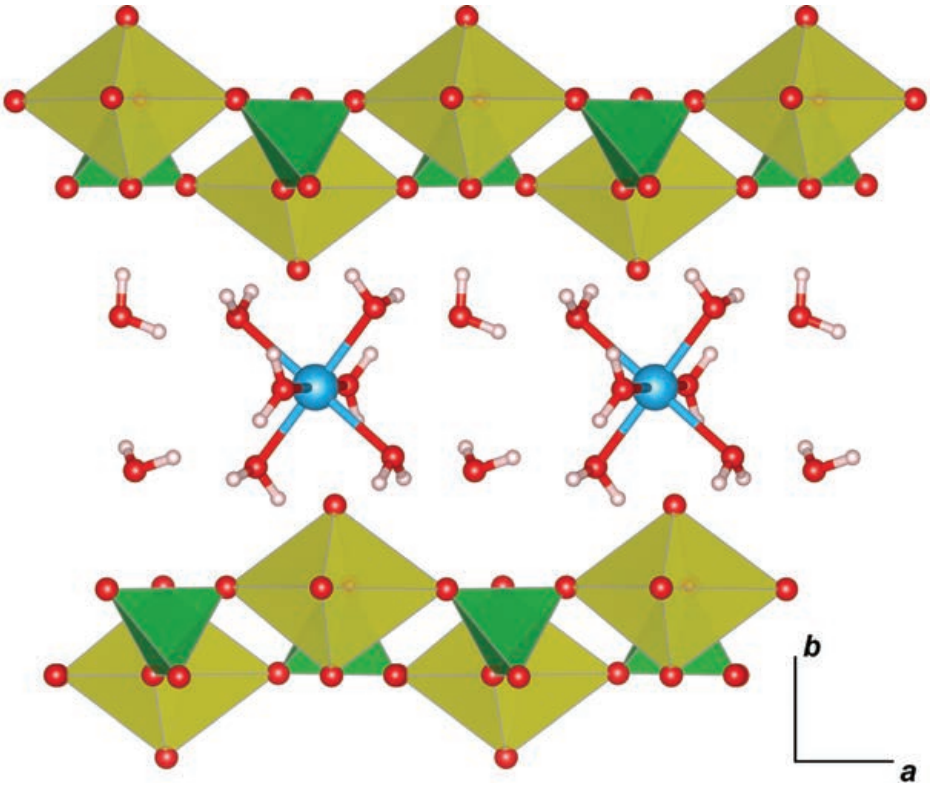

Fig. 3. General view of the structure of bassetite and saléeite perpendicular to (001). Yellow, uranyl polyhedral; green, phosphate tetrahedra; blue, Mg or Fe atoms; red, oxygen atoms; white, hydrogen atoms (VESTA 3 software; Momma & Izumi, 2011).

Table 6. Bond-valence table (*vu*) for bassetite.

	Fe*	U	P	H7a	H7b	H8a	H8b	H9a	H9b	H10a	H10b	H11a	H11b	Σ
O1		1.79		0.21										2.00
O2		1.81				0.11								1.92
O3		0.62	1.31				0.20							2.13
O4		0.62	1.25					0.17						2.04
O5		0.73	1.06							0.16				1.95
O6		0.59	1.34											1.93
O7	0.38 x 2↓			0.74	0.75									1.87
O8	0.36x 2↓					0.74	0.74					0.23		2.08
O9	0.28x 2↓							0.74	0.73		0.13			1.88
O10					0.22					0.74	0.74		0.16	1.86
O11									0.20			0.72	0.74	1.66
Σ	2.04	6.16	4.96	0.95	0.97	0.85	0.95	0.91	0.93	0.90	0.87	0.95	0.90	

*Calculated according to a site-occupancy of 0.64 Fe^{2+} and 0.36 Mg.

nováčekite II), $Co[(UO_2)(PO_4)]_2(H_2O)_{10}$, $Ni[(UO_2)(PO_4)]_2(H_2O)_{10}$ (Locock *et al.,* 2004), and as the mineral rauchite ($Ni[(UO_2)(AsO_4)]_2(H_2O)_{10}$) (Pekov *et al*., 2012). Electron-microprobe analyses performed on rauchite (Pekov *et al*., 2012), metalodevite (Plášil *et al*., 2010b), metakirchheimerite (Plášil *et al*., 2009) and metarauchite (Plášil *et al*., 2010a) indicate that solid-solution series exist between the Mg-, Fe-, Co-, Ni- and Zn-end-members of the autunite and meta-autunite groups.

5.2. The water content of autunite-group minerals

As reviewed by Locock *et al.* (2004), synthetic phases and minerals of the autunite group show some general features: the dodecahydrate compounds ($12H_2O$) have a triclinic pseudo-monoclinic cell, the decahydrate compounds ($10H_2O$) are monoclinic pseudo-orthorhombic (space group $P2_1/n$ or $I2/m$), and the octahydrate ($8H_2O$) compounds are triclinic. Table 8 lists all autunite-group

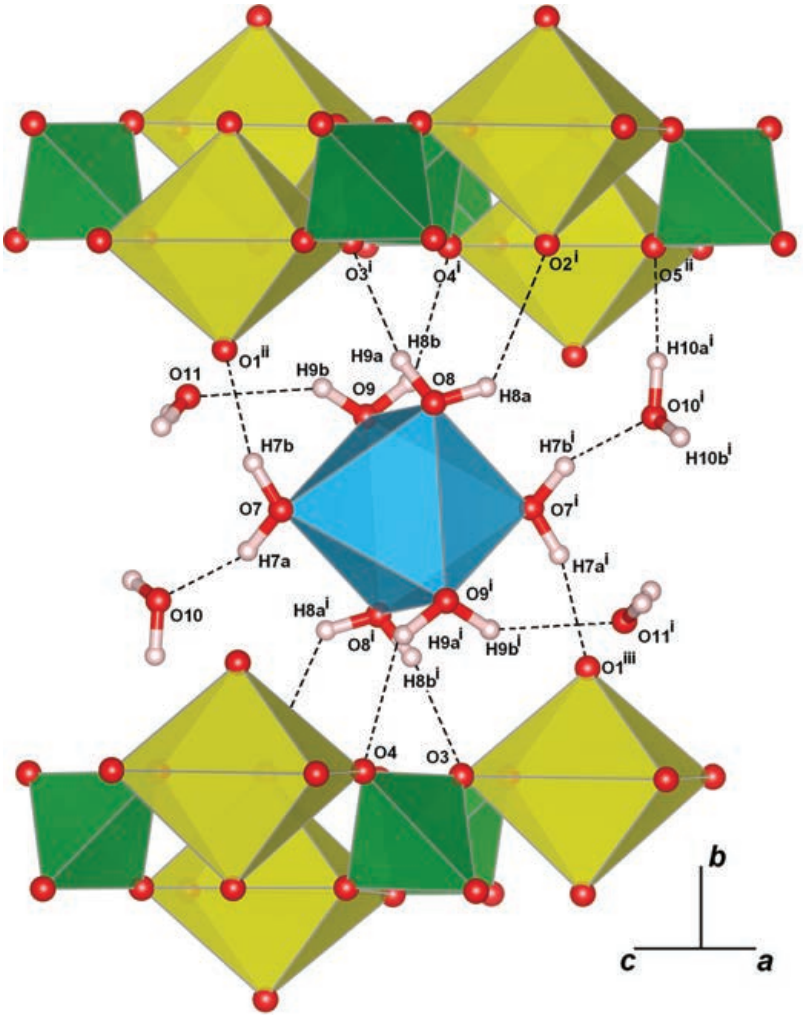

Fig. 4. H-bonds network in the structure of bassetite and saléeite, viewed perpendicular to (101). Symmetry codes: (i) $-x, -y, -z$; (ii) $-x + 1/2, y + 1/2, -z + 1/2$; (iii) $x-1/2, -y-1/2, z-1/2$ (VESTA 3 software; Momma & Izumi, 2011).

Table 7. Bond-valence table (vu) for saléeite from Shinkolobwe, DRC.

	Mg*	U	P	H7a	H7b	H8a	H8b	H9a	H9b	H10a	H10b	H11a	H11b	Σ
O1		1.71		0.22										1.93
O2		1.74				0.10								1.84
O3		0.63	1.23				0.21							2.06
O4		0.62	1.24					0.20						2.06
O5		0.63	1.28							0.12				2.03
O6		0.66	1.19											1.86
O7	0.40x 2↓			0.74	0.74									1.88
O8	0.39 x 2↓					0.75	0.75					0.23		2.11
O9	0.30 x 2↓							0.74	0.74		0.13			1.92
O10					0.23					0.75	0.74		0.17	1.89
O11									0.23			0.74	0.74	1.72
Σ	2.18	5.99	4.94	0.95	0.97	0.85	0.96	0.94	0.97	0.87	0.88	0.97	0.91	

*Calculated according to a site-occupancy of 0.97 Mg and 0.03 Fe^{2+}.

compounds containing magnesium or other divalent metal cations. To date, no dodecahydrate compounds of this group have been reported in nature, and no structural data are available for natural octahydrate phases, which is certainly due to the much worse quality of the crystals passed through a dehydration process. The compounds listed in Table 8 include hypothetical species (in *italics*) and species for which some modifications should be considered (in **bold**).

Table 8. List of minerals from the autunite and meta-autunite groups containing magnesium or other divalent metal cations.

Mineral name	Formula	S.G.	a (Å)/a (°)	b (Å)/p (°)	c (Å)/y (°)	Ref
Torbernite	$Cu[(UO_2)(PO4)]2(H2O)_{12}$	*P4/nnc*	7.03/90	7.03/90	20.81/90	1
Zeunerite	$Cu[(UO_2)(A_SO4)]_2(H_2O)_{12}$	*P4/nnc*	7.18/90	7.18/90	20.86/90	1
Metatorbernite	$Cu[(UO_2)(PO_4)]_2(H_2O)_8$	*P4/n*	6.98/90	6.98/90	17.35/90	1
Metazeunerite	$Cu[(UO_2)(AsO_4)]_2(H_2O)_8$	*P4/n*	7.11/90	7.11/90	17.42/90	1
Saléeite	$Mg[(UO_2)(PO_4)]_2(H_2O)_{l0}$	$P2_1/n$	6.95/90	19.94/90.6	6.97/90	2, 4
nováčekite II	$Mg[(UO_2)(AsO_4)]_2(H_2O)_{10}$	$P2_1/n$	7.13/90	20.08/90.6	7.15/90	3
Bassetite	$Fe[(UO_2)(PO_4)]_2(H_2O)_{10}$	$P2_1/n$	6.96/90	20.04/90.5	6.97/90	4
Kahlerite	$Fe[(UO_2)(AsO_4)]_2(H_2O)_{10}$	*Q*	14.3/90	14.3/90	21.8/90	5, 6
Lehnerite	$Mn[(UO_2)(PO_4)]_2(H_2O)_{10}$	*I2/m*	6.96/90	20.37/91. 0	6.97/90	3, 7
Lehnerite-As	$Mn[(UO_2)(AsO_4)]_2(H_2O)_{10}$	-	-	-	-	-
Kirchheimerite-P	$Co[(UO_2)(PO_4)]_2(H_2O)_{10}$	$P2_i/n$	6.94/90	i9.93/90.4	6.96/90	3
Kirchheimerite	$Co[(UO_2)(AsO_4)]_2(H_2O)_{10}$	-	-	-	-	-
Rauchite-P	$Ni[(UO_2)(PO_4)]_2(H_2O)_{10}$	$P2_1/n$	6.95/90	19.82/90.4	6.97/90	3
Rauchite	$Ni(UO_2)(AsO_4)]_2(H_2O)_{10}$	*I*-1	7. 10/92. 4	7.13/94.9	19.96/90.4	8
Lodèvite-P	$Zn[(UO_2)(PO_4)]_2(H_2O)_{10}$	-	-	-	-	-
Lodèvite	$Zn[(UO_2)(AsO_4)]_2(H_2O)_{10}$	-	-	-	-	-
Metasaléeite	$Mg[(UO_2)(PO_4)]_2(H_2O)_8$	*Q*	7.22/90	7.22/90	17.73/90	9
Metanováčekite	$Mg[(UO_2)(AsO_4)]_2(H_2O)_8$	*Q*	7.16/90	7.16/90	8.58/90	6
Metabassetite	$Fe[(UO_2)(PO_4)]_2(H_2O)_8$	-	-	-	-	-
Metakahlerite	$Fe[(UO_2)(AsO_4)]_2(H_2O)_8$	*P*-1	7.21/75.4	9.82/84.0	13.27/81.8	3
Metalehnerite	$Mn[(UO_2)(PO_4)]_2(H_2O)_8$	-	-	-	-	7
Metalehnerite-As	$Mn[(UO_2)(AsO_4)]_2(H_2O)_8$	*P*-1	7.22/75.0	9.91/84.1	13.33/82.0	3, 7
Metakirchheimerite-P	$Co[(UO_2)(PO_4)]_2(H_2O)_8$	-	-	-	-	-
Metakirchheimerite	$Co[(UO_2)(AsO_4)]_2(H_2O)_8$	*P*-1	7.19/75.5	9.77/84.0	13.23/81.6	3
Metarauchite-P	$Ni[(UO_2)(PO_4)]_2(H_2O)_8$	-	-	-	-	-
Metarauchite	$Ni[(UO_2)(AsO_4)]_2(H_2O)_8$	*P*-1	7.19/75.8	9.71/83.9	13.20/81.6	10
Metalodèvite-P	$Zn[(UO_2)(PO_4)]_2(H_2O)_8$	-	-	-	-	-
Metalodèvite	$Zn[(UO_2)(AsO_4)]_2(H_2O)_8$	*P*-1	7.19/75.5	9.77/84.1	13.24/81.7	11, 12

Q = tetragonal. Italic, hypothetical end-members; bold, species with questionable hydration state indication or unit-cell parameters (see text). References: 1, Locock & Burns (2003); 2, Yakubovich et al. (2008); 3, Locock *et al.* (2004); 4, this study; 5, Meixner (1953); 6, Walenta (1964); 7, Mücke (1988); 8, Pekov *et al.* (2012); 9, Cassedanne *et al.* (1986); 10, Plášil *et al.* (2010a); 11, Agrinier *et al.* (1972); 12, Plášil *et al.* (2010b).

Bassetite is reported as probably containing eight water molecules (Hallimond, 1915; Frondel, 1954), despite the fact that bassetite was supposed to be isostructural with saléeite, which has generally been reported as containing ten water molecules (Piret & Deliens, 1980). Considering all observations given above and the refinement of the structure of type-locality bassetite in the present work, it is clear that the formula of bassetite is $Fe^{2+}[(UO_2)(PO_4)]_2(H_2O)_{10}$.

Kahlerite, $Fe^{2+}[(UO_2)(AsO_4)]_2(H_2O)_{8\text{-}12}$, is described as having a tetragonal symmetry and a water content of eight or twelve water molecules per formula unit (*pfu)* (Meixner, 1953; Walenta, 1964). Considering the general isotypism between uranyl phosphates and arsenates, and between the Mg and Fe end-members, kahlerite is the arsenate-equivalent of bassetite and its composition should be reported as $Fe^{2+}[(UO_2)(AsO_4)]_2(H_2O)_{10}$. The unit-cell parameters of kahlerite should be very close to those of bassetite and nováčekite II ($P2_1/c$; Locock *et al*., 2004).

Lehnerite, $Mn[(UO_2)(PO_4)]_2(H_2O)_8$, was described by Mücke (1988) as a structural analogue of bassetite, which was considered at that time as containing eight water molecules *pfu.* Our results for bassetite raise the question of whether lehnerite is the Mn-equivalent of decahydrate bassetite, or actually metalehnerite. Mücke (1988) did not perform thermal analyses and therefore deduced the water content of lehnerite from electron-microprobe analysis, which is not the optimal technique to estimate the water content in highly hydrated minerals with sheet structure. Unit-cell parameters of lehnerite were calculated according to those of bassetite reported by Frondel (1954): a = 7.04(2), b = 17.16(4), c = 6.95(2) Å and β = 90.18(2)° ($P2_1/c$) (Mücke, 1988). Locock *et al.* (2004) synthesized the analogue of decahydrate lehnerite (*MnUP10)* and refined its crystal structure with the unit-cell parameters a = 6.96, b = 20.38, c = 6.98 Å and β = 91.02(2)° (*I2/m*). These values are very close to those of bassetite, saléeite and nováčekite II, despite the difference in reported space group (*I2/m vs.* $P2_1/n$). The modification of the space group is explained by a different arrangement of the water molecules in the structure of *MnUP10,* due to the ionic radius of $^{[6]}Mn^{2+}$ (0.830 A; Shannon, 1976), which is larger than those of Fe and Mg (Locock *et al.*, 2004). Comparison between the X-ray powder diffraction pattern of lehnerite (International Center for Diffraction

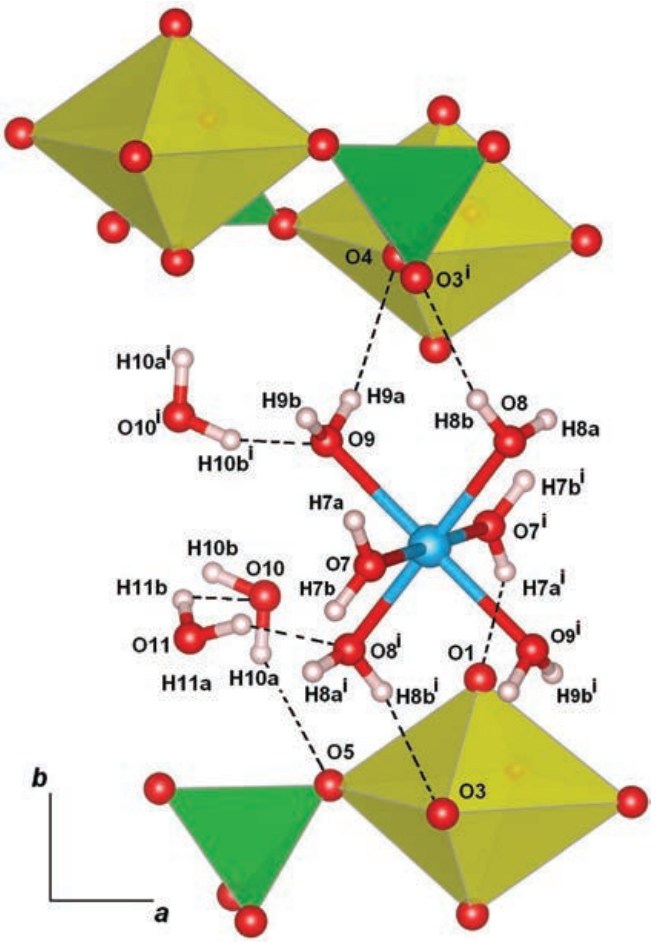

Fig. 5. H-bonds network in the structure of bassetite and saléeite, viewed along the *c* axis.. Symmetry code: (i) -x, -y, -*z* (VESTA 3 software; Momma & Izumi, 2011).

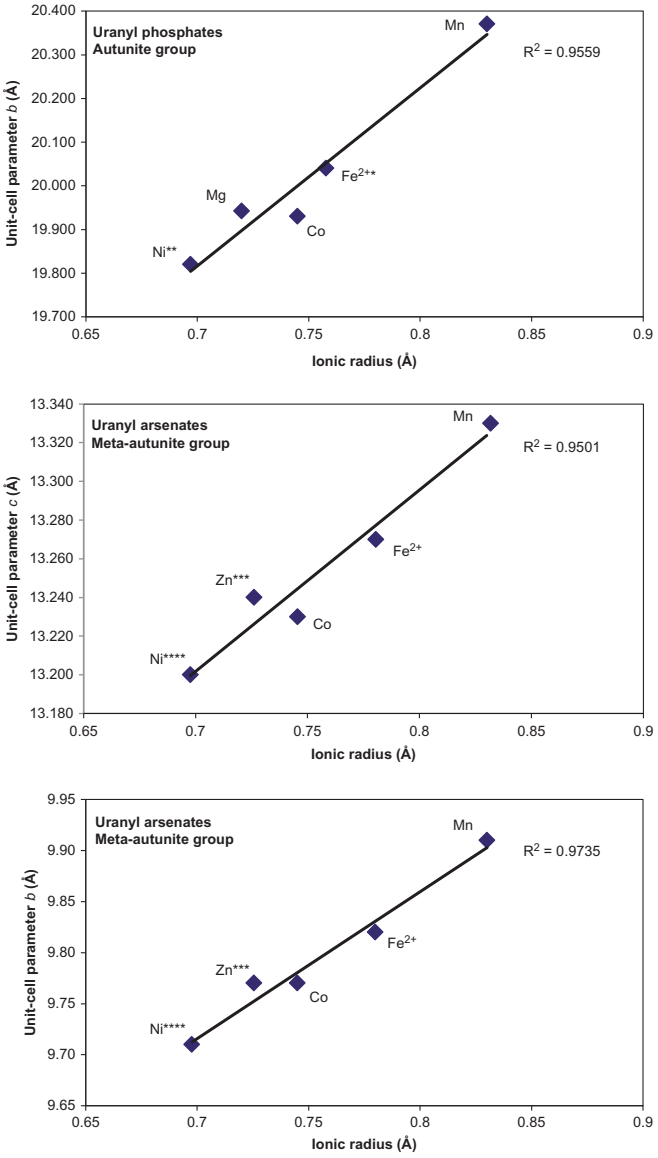

Fig. 6. Diagram showing the correlation between unit-cell parameters and ionic radii of the octahedral bivalent cations. (a) Uranyl phosphates of the autunite group; (b) and (c) uranyl arsenates of the meta-autunite group. Some ionic radii are calculated according to mixed occupancy: * (0.64 Fe, 0.36 Mg); ** (0.78 Ni, 0.20 Mg, 0.01 Co, 0.01 Zn); *** (0.77 Zn, 0.11 Fe, 0.06 Mg, 0.05 Al); **** (0.85 Ni, 0.13 Co, 0.02 Mg). Sources: see Table 8.

Data, ICDD, 2012), PDF card 00-045-1421) and that of *MnUP10* (PDF card 00-014-6736) indicates that these two phases are not identical. However, the X-ray powder diagram of lehnerite is very close to that of synthetic $Mn[(UO_2)(AsO_4)]_2(H_2O)_8$ (*MnUAs8,* PDF card 04-014-6740) reported by Locock *et al.* (2004). These observations indicate that lehnerite initially studied by Mücke (1988) should actually be redefined as metalehnerite.

Finally, the unit-cell parameters reported for metasaléeite (Cassedanne *et al.*, 1986) and metanovacekite (Walenta, 1964) are also questionable. Both minerals are reported to be tetragonal, whereas all the other synthetic compounds of the meta-autunite group are triclinic (Locock *et al.*, 2004). It could be assumed that the tetragonal symmetry reported for metasaléeite and metanovacekite is in fact pseudo-tetragonal, and that the true symmetry is actually triclinic.

5.3. Variation of unit-cell parameters

The unit-cell parameters of members (with magnesium and other divalent metal cations) of the autunite and meta-autunite groups are affected by the nature of the tetragonal cations (P or As) and of the octahedral cations (Table 8). The influence of the tetrahedral cations is revealed by the unit-cell parameters defining the autunite-type sheet (*a* and *b* for the autunite group, *a* and *c* for the meta-autunite group). The tetrahedral cations also affect to a lesser extent the parameter along the stacking direction of the sheets (usually less than 0.1% increase when P is replaced by As).

The nature of the octahedral cations does not affect the unit-cell parameters parallel to the autunite-type sheet (Table 8). However, it strongly affects the

crystallographic parameter perpendicular to the stacking of the sheet. Figure 6 shows the correlation between unit-cell parameters and ionic radii of the octahedral divalent cations (ionic radius from Shannon, 1976). As unit-cell parameters are not available for some species, Figure 6 shows only the correlation for uranyl phosphates of the autunite group (Fig. 6a), and correlation for the uranyl arsenates of the meta-autunite group (Fig. 6b and c). The correlation is extremely good in all cases, indicating that ionic radius of the octahedral cation is the main factor that affects the distance between two successive sheets (considering the same hydration state). Using these correlations, the unit-cell parameters perpendicular to the stacking sequence can be obtained for the *P*-analogue of *lodèvite* (b = 19.98 Å) and for metanovacekite (b = 9.74 and c = 13.22 Å).

Acknowledgements: Many thanks to Stéphane Puccio for the loan of the saléeite specimen. We are also grateful to Roger Warin for the photomicrographs of the samples. Jakub Plášil as well as an anonymous reviewer are thanked for their insightful comments that helped improve the manuscript. FD thanks the FRS-F.N.R.S. (Belgium) for a FRIA PhD grant n° 93482.

References

Agilent Technologies. (2012): CrysAlis CCD and CrysAlis RED. Oxford Diffraction Ltd., Yarnton, Oxfordshire, UK.

Agrinier, H., Chantret, F., Geffroy, J., Héry, B., Bachet, B., Vachey, H. (1972): Une nouvelle espèce minérale: la méta-lodèvite (arséniate hydraté d'uranium et de zinc). *Bull. Soc. Fr. Minéral. Cristallogr.*, **95**, 360–364.

Beintema, J. (1938): On the composition and crystallography of autunite and the meta-autunite. *Recl. Trav. Chim. Pays-Bas*, **57**, 155–175.

Brown, I.D. & Altermatt, D. (1985): Bond-valence parameters obtained from a systematic analysis of the inorganic crystal structure database. *Acta Cryst.*, **B41**, 244–247. with updated parameters from http://www.ccp14.ac.uk/ccp/web-mirrors/i_d_brown/.

Buck, E.C., Brown, N.R., Dietz, N.L. (1996): Contaminant uranium phases and leaching at the Fernald site in Ohio. *Envir. Sci. Tech.*, **30**, 81–88.

Burns, P.C., Ewing, R.C., Hawthorne, F.C. (1997): The crystal chemistry of hexavalent uranium: polyhedron geometries, bond-valence parameters, and polymerization of polyhedra. *Can. Mineral.*, **35**, 1551–1570.

Cassedanne, J.P., Cassedanne, J.O., De Carvalho, H.F. (1986): Loellingite, uraninite, and their alteration products in the pegmatite from Urucum (Minas Gerais, Brazil). *An. Acad. Bras. Cienc.*, **58**, 249–266.

Dal Bo, F., Hatert, F., Baijot, M., Philippo, S. (2015): Crystal structure of arsenuranospathite from Rabejac, Lodève, France. *Eur. J. Mineral.*, **27**, 589–597.

Frondel, C. (1951): Studies of uranium minerals (IX): saléeite and nováčekite. *Am. Mineral.*, **36**, 680–686.

Frondel, C. (1954): Bassetite and uranospathite. *Mineral. Mag.*, **30**, 343–353.

Fuller, C.C., Bargar, J.R., Davis, J.A., Piana, M.J. (2002): Mechanisms of uranium interactions with hydroxyapatite: implications for groundwater remediation. *Envir. Sci. Tech.*, **36**, 158–165.

Grabias, E., Gładysz-Płaska, A., Książek, A., Majdan, M. (2014): Efficient uranium immobilization on red clay with phosphates. *Environ. Chem. Lett.*, **12**, 297–301.

Hallimond, A.F. (1915): On bassetite and uranospathite, new species hitherto classed as autunite. *Mineral. Mag.*, **17**, 221–236.

ICDD. (2012): *WebPDF-4 +*. International centre for diffraction data. Newtown Square, Pennsylvania, USA.

Jerden, J.L. & Sinha, A.K. (2003): Phosphate based immobilization of uranium in an oxidizing bedrock aquifer. *Appl. Geochem.*, **18**, 823–843.

Krivovichev, S.V. & Plášil, J. (2013): Mineralogy and crystallography of uranium. *in* ''Uranium - Cradle to Grave'', P.C. Burns and G.E. Sigmon, eds. Short Course Series, **43**, Mineralogical Association of Canada, Québec, 15–119.

Locock, A.J. & Burns, P.C. (2003): Crystal structures and synthesis of the copper-dominant members of the autunite and meta-autunite groups: torbernite, zeunerite, metatorbernite and metazeunerite. *Can. Mineral.*, **41**, 489–502.

Locock, A.J., Burns, P.C., Flynn, T.M. (2004): Divalent transition metals and magnesium in structures that contain the autunite-type sheet. *Can. Mineral.*, **42**, 1699–1718.

Meixner, H. (1953): Kahlerit, ein neues Mineral der Uranglimmergruppe, aus der Huttenberger Erzlagerstatte. *Der Karinthin*, **23**, 277–280.

Miller, S.A. & Taylor, J.C. (1986): The crystal structure of saleeite, $Mg[UO_2PO_4].10H_2O$. *Z. Kristallogr.*, **177**, 247–253.

Momma, K. & Izumi, F. (2011): VESTA 3 for three-dimensional visualization of crystal, volumetric and morphology data. *J. Appl. Crystallogr.*, **44**, 1272–1276.

Mrose, M. (1950): Studies of uranium minerals (III): saléeite from Schneeberg, Saxony. *Am. Mineral.*, **35**, 525–530.

Mücke, A. (1988): Lehnerite $Mn[UO_2|PO_4]_2{\cdot}8H_2O$, as a new mineral from the pegmatite of Hagendorf/Oberpfalz. *Der Aufschluss*, **39**, 209–217.

Murakami, T., Ohnuki, T., Isobe, H., Sato, T. (1997): Mobility of uranium during weathering. *Am. Mineral.*, **82**, 888–899.

Pekov, I.V., Levitskiy, V.V., Krivovichev, S.V., Zolotarev, A.A., Bryzgalov, I.A., Zadov, A.E., Chukanov, N.V. (2012): New nickel-uranium-arsenic mineral species from the oxidation zone of the Belorechenskoye deposit, Northern Caucasus, Russia: I. Rauchite, $Ni(UO_2)_2(AsO_4)_2 \cdot 10H_2O$, a member of the autunite group. *Eur. J. Mineral.*, **24**, 913–922.

Piret, P. & Deliens, M. (1980): Nouvelles données sur la saléeite holotype de Shinkolobwe. *Bull. Minéral.*, **103**, 630–632.

Plášil, J., Čejka, J., Sejkora, J., Hloušek, J., Goliáš, V. (2009): New data for metakirchheimerite from Jáchymov (St. Joachimsthal), Czech Republic. *J. Geosci.*, **54**, 373–384.

Plášil, J., Sejkora, J., Čejka, J., Novák, M., Viñals, J., Ondruš, P., Veselovský, F., Škácha, P., Jehlička, J., Goliáš, V., Hloušek, J. (2010a): Metarauchite $Ni(UO_2)_2(AsO_4)_2.8H_2O$ from Jáchymov, Czech Republic, and Schneeberg, Germany: A new member of the autunite group. *Can. Mineral.*, **48**, 335–350.

Plášil, J., Sejkora, J., Čejka, J., Škácha, P., Goliáš, V., Ederová, J. (2010b): Characterization of phosphate-rich metalodèvite from Příbram, Czech Republic. *Can. Mineral*., **48**, 113–122.

Roh, Y., Lee, S.R., Choi, S.K., Elless, M.P., Lee, S.Y. (2000): Physicochemical and mineralogical characterization of uranium contaminated soils. *Soil Sediment Contam*., **9**, 463–486.

Schoep, A. (1939): Splijtingen, Corrosie-figuren en monokliene Symmetrie van Saléeiet; epitaxie op Metatorberniet. *Meded. Kl. Wetens. Kon Vlaamsche Acad. Wetens Lett*., 65–70.

Shannon, R.D. (1976): Revised effective ionic radii and systematic studies of interatomic distances in halide and chalcogenides. *Acta Cryst*., **A32**, 751–767.

Sheldrick, G.M. (2008): A short history of SHELX. *Acta Cryst*., **A64**, 112–122.

Thoreau, J. & Vaes, J.F. (1932): La saléite, nouveau minéral uranifère. *Bull Soc. Belge Géol*., **42**, 96–99.

Vochten, R., De Grave, E., Pelsmaekers, J. (1984): Mineralogical study of bassetite in relation to its oxidation. *Am. Mineral*., **69**, 967–978.

Walenta, K. (1964): Beiträge zur Kenntnis seltener Arsenatmineralien unter besonderer Berücksichtigung von Vorkommen des Schwarzwaldes. I. *Tschermaks Mineral. Petrogr. Mitt*., **9**, 111–174.

Wilson, A.J.C. (1992): International Tables for X-ray Crystallography. Vol. C, Kluwer Academy Press, London, 883 p.

Yakubovich, O.V., Steele, I.M., Atencio, D., Menezes, L.A., Chukanov, N.V. (2008): Crystal structure of the $(Mg,Fe)[UO_2(P,As)O_4]_2.10H_2O$ solid solution - a novel mineral variety of saléeite. *Crystallogr. Rep*., **53**, 764–770.

Received 22 October 2015
Modified version received 21 December 2015
Accepted 22 December 2015